Transition Met Chem (2013) 38:641–648
DOI 10.1007/s11243-013-9732-6

Synthesis, structural characterisation and catalytic application of dichloro(η^6-*p*-cymene){diphenyl(3-methyl-2-indolyl)phosphine} ruthenium(II) in the transfer hydrogenation of ketones

Yu-Ying Kuo · Mairi F. Haddow · Ashley L. Jamieson · Gareth R. Owen

Received: 30 April 2013 / Accepted: 15 May 2013 / Published online: 28 May 2013

Abstract The synthesis and investigation of ruthenium complexes containing the relatively unexplored ligand, diphenyl-2-(3-methyl)indolylphosphine, is presented herein. The complexes $[RuCl_2\{PPh_2(C_9H_8N)\}_3]$, $[Ru_2(\mu\text{-}Cl)_3(Cl)(MeCN)\{PPh_2(C_9H_8N)\}_4]$ and $[RuCl_2(\eta^6\text{-}p\text{-cymeme})\{PPh_2(C_9H_8N)\}]$ have been studied. Single crystals of the latter two complexes have been prepared and investigated by X-ray crystallography. A detailed examination of $[RuCl_2(\eta^6\text{-}p\text{-cymeme})\{PPh_2(C_9H_8N)\}]$ has been carried out. This complex was found to be an active catalyst in the catalytic transfer hydrogenation of ketones.

Introduction

There is currently great interest in ligands which contain N–H functional groups and their ability to participate intimately within transformations at the metal centre. Such cooperation between ligand and metal centre has certainly led to substantial improvements in many catalytic transformations [1–3]. The role of N–H functional groups in catalysis has recently been examined in great detail by Ding [4]. One significant area of interest has been the development of phosphorus ligands containing NH functionalities. Perhaps one of the most important and early contributions to this field is the work carried out by Noyori and co-workers, in which they introduced metal–ligand bifunctional catalysts for asymmetric hydrogenation reactions [5–7]. Many ruthenium complexes which are active hydrogenation and transfer hydrogenation catalysts are now known [8–31].

For some time now, we have been interested in hydrogenation reactivity as a means of exploring potential ligand cooperation effects. Our investigations have focused on the close proximity of various functional groups to the transition metal centres. Much of our work has involved B–H functional groups [32–42], though we have also investigated a relatively unexplored phosphorus ligand containing an N–H functional group [43]. In this report, we prepared some group nine complexes containing the ligand, diphenyl-2-indolylphosphine (**L**) (Fig. 1). This ligand, along with some related phosphine compounds containing the same indolyl functional group, was originally developed by Browning [44]. To date, there have only been a handful of complexes containing **L** [43–47], with the only ruthenium complexes based on the precursor $Ru_3(CO)_{12}$ [45]. In some of these complexes, the ligand coordinates to the metal centre via the phosphorus atom, and the pendant NH group was found to undergo strong hydrogen-bonding interactions with halide co-ligands [44, 46]. Additionally, there are a number of derivative ligands known [47–58] which have been utilised as co-ligands in catalytic applications such as Suzuki–Miyaura coupling of aryl chlorides [50], asymmetric hydrogenation [51, 52], hydroformylation [52] and allylic alkylation reactions [53, 54]. We also introduced the η^6-coordination mode for **L** [43].

The coordination chemistry of **L** itself however remains limited, and we therefore wish to report the synthesis of the first mononuclear ruthenium complexes containing this ligand along with some preliminary results of the catalytic performance of a complex in the transfer hydrogenation of ketones.

Y.-Y. Kuo · M. F. Haddow · A. L. Jamieson · G. R. Owen (✉)
The School of Chemistry, Cantock's Close, Bristol, UK
e-mail: gareth.owen@bristol.ac.uk

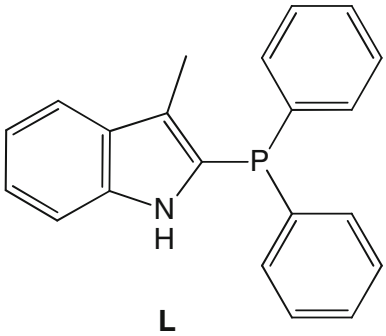

Fig. 1 Diphenyl-2-indolylphosphine, **L**

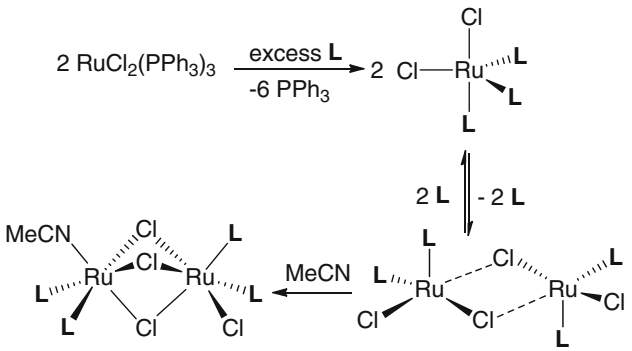

Scheme 1 Synthesis and subsequent reactivity of $[RuCl_2(\mathbf{L})_3]$ with MeCN

Results and discussion

A wide range of ruthenium complexes bearing ligands with N–H groups are known to provide effective catalysts within transfer hydrogenation reactions [1–3, 59–62]. With that in mind, we set out to explore synthetic methods towards new ruthenium complexes containing **L**. Our initial starting point was the reaction of **L** with common precursors such as $[RuCl_2(COD)]_n$ and $[RuCl_2(DMSO)_4]$. The addition of an excess of **L** to a solution of the former compound in various solvents revealed very little indication of phosphine coordination to the ruthenium centre even under forcing conditions, as determined by $^{31}P\{^1H\}$ NMR spectroscopy.[1] Reactions involving the latter precursor consistently gave complicated reaction mixtures, with at least 5 coordinated phosphorus ligand environments observed by $^{31}P\{^1H\}$ NMR spectroscopy. Our attempts to isolate pure samples from these mixtures were unsuccessful. When $[RuCl_2(PPh_3)_3]$ was reacted with a fivefold excess of **L** in toluene solvent, two broad signals were observed in the $^{31}P\{^1H\}$ NMR spectrum at 28.4 and 35.3 ppm (δ toluene, unlocked), respectively, along with signals corresponding to the eliminated free triphenylphosphine (Scheme 1). These two signals are very similar to the pattern obtained in the spectrum of related complexes containing three phosphorus ligands including the starting material [63–67]. The species was given the tentative assignment $[RuCl_2\mathbf{L}_3]$, the two chemical environments originating from the trigonal bipyramidal complex. As the spectrum was broad, it is likely that Berry pseudo-rotation is occurring on the NMR timescale, although exchange between PPh_3 and **L** at ruthenium cannot be ruled out. Our attempts to isolate a pure sample of $[RuCl_2\mathbf{L}_3]$ from the mixture proved unsuccessful. During these attempts, we obtained single crystals of a different compound from an acetonitrile solution. An X-ray single-crystallographic analysis of the crystals revealed its identity to be a dinuclear complex with the composition of $[Ru_2Cl_4(NCMe)\mathbf{L}_4]$ (Fig. 2).

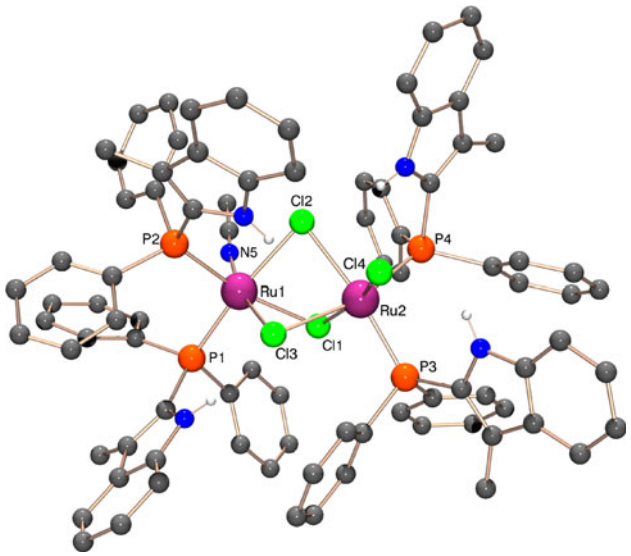

Fig. 2 Crystal structure of $[Ru_2Cl_4(NCMe)\mathbf{L}_4]\cdot 2\ CHCl_3$, solvent molecules and hydrogen atoms {except for hydrogen atoms on indolyl NH group} has been omitted for clarity. Selected bond distances (Å) and angles (°); Ru(1)–N(5) 2.000(6), Ru(1)–P(1) 2.3060(17), Ru(1)–P(2) 2.3064(16), Ru(1)–Cl(3) 2.4124(15), Ru(1)–Cl(1) 2.4477(15), Ru(1)–Cl(2) 2.4618(15), Ru(2)–P(3) 2.2751(16), Ru(2)–P(4) 2.2795(17), Ru(2)–Cl(1) 2.3721(15), Ru(2)–Cl(4) 2.4151(16), Ru(2)–Cl(2) 2.5029(15), Ru(2)–Cl(3) 2.5483(15), N(5)–Ru(1)–P(1) 90.08(16), N(5)–Ru(1)–P(2) 93.27(16), P(1)–Ru(1)–P(2) 100.77(6), P(1)–Ru(1)–Cl(3) 98.84(6), P(2)–Ru(1)–Cl(3) 94.83(5), N(5)–Ru(1)–Cl(1) 88.15(16), P(1)–Ru(1)–Cl(1) 91.76(6), Cl(3)–Ru(1)–Cl(1) 81.65(5), N(5)–Ru(1)–Cl(2) 85.98(16), P(2)–Ru(1)–Cl(2) 88.48(5), Cl(3)–Ru(1)–Cl(2) 83.60(5), Cl(1)–Ru(1)–Cl(2) 79.11(5), P(3)–Ru(2)–P(4) 100.21(6), P(3)–Ru(2)–Cl(1) 91.08(5), P(4)–Ru(2)–Cl(1) 95.91(6), P(3)–Ru(2)–Cl(4) 95.02(6), P(4)–Ru(2)–Cl(4) 98.96(6), P(4)–Ru(2)–Cl(2) 83.64(6), Cl(1)–Ru(2)–Cl(2) 79.73(5), Cl(4)–Ru(2)–Cl(2) 93.05(5), P(3)–Ru(2)–Cl(3) 95.76(5), Cl(1)–Ru(2)–Cl(3) 80.36(5), Cl(4)–Ru(2)–Cl(3) 82.87(5), Cl(2)–Ru(2)–Cl(3) 80.06(5)

[1] Mixtures containing $[RuCl_2(COD)]_n$ and 2 equivalents of **L** were heated to reflux in MeCN for several days. The $^{31}P\{^1H\}$ NMR spectrum of the reaction mixture revealed mostly free ligand with only traces of a new species at 13.9 ppm (<10 %) which was likely to correspond to the target product, $RuCl_2(COD)\mathbf{L}$. The lack of reactivity is presumably due to the inability of **L** to break the chloride bridges in the polymeric starting material. Due the this lack of reactivity, the route was not further explored.

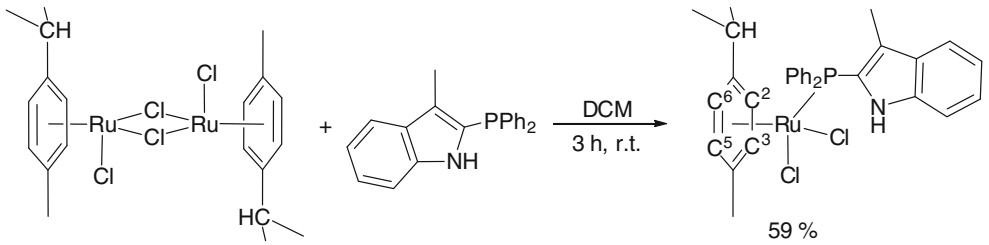

Scheme 2 Synthesis of $[RuCl_2\{\eta^6\text{-}p\text{-cymene}\}\mathbf{L}]$

The structure revealed that the coordination spheres at the ruthenium metal centres were both based on distorted octahedral geometries, each comprising of 3 bridging chlorides, 2 ligands (**L**) and one additional terminal chloride on one ruthenium centre or a coordinated acetonitrile ligand on the other. The formation of face-sharing bioctahedral Ru(II) halide complexes has previously been observed in the literature [68–71]. As shown in Fig. 2, the Ru–Cl bonds *trans* to phosphorus [Ru(1)–Cl(1) = 2.4477(15) Å, Ru(1)–Cl(2) = 2.4618(15) Å, Ru(2)–Cl(2) = 2.5029(15) Å, Ru(2)–Cl(3) = 2.5483(15) Å] are longer than those *trans* to the terminal chloride [Ru(2)–Cl(1) = 2.3720(15) Å] or the acetonitrile ligand [Ru(1)–Cl(3) = 2.4124(15) Å]. This is due to the larger *trans* influence of the phosphorus donor ligands. The Ru–P bond lengths are in the range 2.2751(16)–2.3064(16) Å. It is worth noting that the NH groups of the indolyl units are all orientated towards the chloride ligands within the complex where the shortest NH···Cl distance is 2.286(1) Å [involving the NH group of P(1) and the bridging chloride Cl(3)]. These intramolecular interactions may be strong enough to hinder the rotation of the Ru–P bond, as found in other examples in the literature [46].

The crystal structure gives some insight into the reaction coordinate from $[RuCl_2\mathbf{L}_3]$ to $[Ru_2Cl_4(NCMe)\mathbf{L}_4]$ (Scheme 1). Based on previous reported examples [71], it is likely that the 14 valence electron intermediate complex, "$Ru(II)Cl_2\mathbf{L}_2$", is formed in solution via the elimination of one equivalent of **L** from the complex. Two of these unsaturated complexes then associate, forming halide bridges and the resulting halide-bridged bimetallic complex subsequently receives an acetonitrile molecule to furnish the electronically saturated face-sharing dimeric complex observed in the structure. Mass spectroscopy (ESI^+) of the crystalline material showed peaks corresponding to the $[RuCl\mathbf{L}_2]^+$ and $[RuCl(MeCN)\mathbf{L}_2]^+$ fragments. On the other hand, the $^{31}P\{^1H\}$ and ^1H NMR spectra of the crystalline material revealed a number of poorly resolved signals, indicating that a mixture of species is reformed when the product is placed in solution. Such difficulty in determining the correct stoichiometry is clearly a disadvantage and thus renders the product less suitable for catalytic investigations. Furthermore, the formation of halide-bridged bimetallic complexes is often regarded as undesirable for catalytic applications [71, 72].

As an alternative, the complex $[RuCl_2\{\eta^6\text{-}p\text{-cymene}\}\mathbf{L}]$ was targeted. Indeed, this complex was readily obtained via the straightforward addition of one equivalent of **L** to one-half equivalent of the dinuclear precursor $[RuCl_2\{\eta^6\text{-}p\text{-cymene}\}]_2$ in DCM solvent (Scheme 2). After 3 h, a red micro-crystalline solid was isolated in moderate yield following a standard workup (see Experimental Section). The new complex was fully characterised by spectroscopic and analytical techniques. The $^{31}P\{^1H\}$ NMR spectrum consisted of a sharp single peak at 9.48 ppm (δ $CDCl_3$). The IR spectrum of the isolated solid showed bands characteristic of the phosphorus ligand together with a sharp band at 3,289 cm^{-1} which was attributed to the stretching mode of the NH group. Furthermore, mass spectroscopy and elemental analysis were both consistent with the molecular composition of the expected product.

The ^1H and $^{13}C\{^1H\}$ NMR data were consistent with the formation of $[RuCl_2\{\eta^6\text{-}p\text{-cymene}\}\mathbf{L}]$ confirming that **L** and *p*-cymene were present in a 1:1 ratio. In free *p*-cymene, the chemical shifts for all the ring protons are isochronous at 7.32 ppm in ^1H NMR, while their corresponding carbon signals are observed at 126.3 and 129.0 ppm in the $^{13}C\{^1H\}$ NMR spectrum [73]. Upon coordination to the ruthenium centre in $[RuCl_2\{\eta^6\text{-}p\text{-cymene}\}]_2$, the signals are shifted upfield to 5.30 ppm (^1H) and 80.5 ppm (^{13}C) for $C^{3,5}H$ and 5.44 ppm (^1H) and 81.2 ppm (^{13}C) for $C^{2,6}H$, as a result of donation of the π-electrons from the aromatic ring to the metal [74]. The proton and carbon pairs (δ ^1H, $^{13}C\{^1H\}$) in $[RuCl_2\{\eta^6\text{-}p\text{-cymene}\}\mathbf{L}]$ were confirmed and established by the heteronuclear $^1H/^{13}C$ correlation experiments. They were found to be 5.15 ppm (^1H) and 85.7 ppm (^{13}C) for $C^{2,6}H$ and 5.18 ppm (^1H) and 90.7 ppm (^{13}C) for $C^{3,5}H$. Note that in this case, the trend is reversed, the downfield signals we found to correspond to the signals *ortho* to isopropyl group ($C^{2,6}H$) and the upfield signals were identified as the signals *ortho* to methyl group ($C^{3,5}H$). Interestingly, this showed a reverse trend to the corresponding signals for other ruthenium–cymene complexes from the literature [74]. The reason for these observations is currently unknown. There is a small difference in the $^2J_{CP}$ coupling constants of the

cymene carbon and the phosphorus nuclei ($^2J_{CP} = 6$ Hz for $C^{2,6}H$ and $^2J_{CP} = 4$ Hz for $C^{3,5}H$) which is likely to result from the respective P–Ru–C angles. The NH signal was observed at 10.44 ppm in the ^1H NMR spectrum, suggesting its interaction with the chloride ligands. Such interaction might result in the two phenyl groups of the phosphine to be held in one position and preventing the cymene ligand from rotating, as found in a similar complex [$RuCl_2$(*p*-cymene)(phosphine)] [74]. This was further confirmed by a single-crystal diffraction study as outlined below.

Red needle crystals of [$RuCl_2\{\eta^6$-*p*-cymene$\}$**L**] were formed by laying hexane on the top of a concentrated DCM solution of the complex. A single-crystal diffraction study confirmed the expected product. The Ru–C distances for each of the cymene ring carbon atoms range between 2.183(7) and 2.228(7) Å. These are similar to those found for other [$RuCl_2(\eta^6$-cymene)(PR_3)] (PR_3 = organophosphorus ligands) compounds the in literature [74–76]. The Ru(1)–P(1) bond bisects the edge of the C^5 and C^6 atoms in the cymene, in order to reduce the intramolecular repulsions, and has a bond length of 2.3618(19) Å. This is longer than the average distance for Ru–P bond in the [Ru_2Cl_4(MeCN)$\mathbf{L}_4$] structure. Ru–Cl bonds are 2.4152(18) and 2.404(2) Å while angle for Cl(1)–Ru(1)–Cl(2) is 87.43(7)°, similar to those published structures. The N(1) and H(1) in the indolyl group is not orientated to the centre of two chloride ligands but rather points towards just one of them [Cl(1)]. The N(1)–H(1)–Cl(1) angle is 141.4° and the H(1)–Cl(1) distance is 2.434 Å. The corresponding H(1)–Cl(2) distance is 2.813 Å (Fig. 3). The shorter H(1)–Cl(1) distance is within the range of a hydrogen bond.

The cone angle, defined by the average of three half angles of each substituent on the phosphorus atom, has been calculated as 119.56° [77]. The rotation of cymene ligand is prohibited by the fact that the isopropyl group is facing towards the same side as Ru(1)–P(1) bond, as all the others within the literature. This would cause a steric repulsion between the isopropyl group and the closest phenyl group to hinder the rotation of cymene. This supports the evidence obtained from the $^{13}C\{^1H\}$-NMR data.

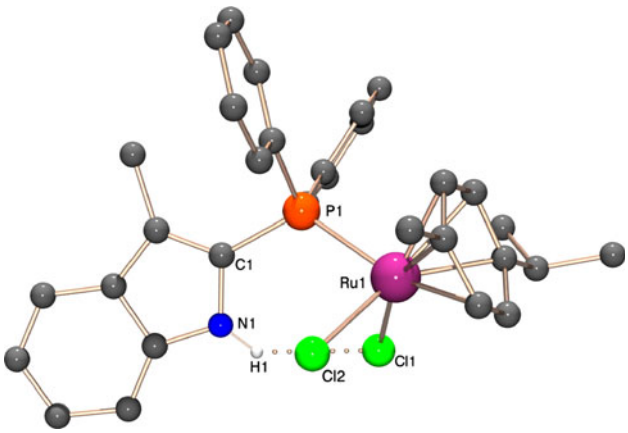

Fig. 3 Crystal structure of [$RuCl_2\{\eta^6$-*p*-cymene$\}$**L**], hydrogen atoms {except for H(1)} has been omitted for clarity. Selected bond lengths (Å) and angles (°); Ru(1)–P(1) 2.3618(19), Ru(1)–Cl(1) 2.4152(18), Ru(1)–Cl(2) 2.404(2), C(1)-P(1) 1.806(8), Cl(1)–Ru(1)–Cl(2) 87.43(7), C(1)-P(1)-Ru(1) 118.8(3)

Table 1 Transfer hydrogenation of ketones using complexes **1**, **2**, **6** and **7** with 0.2 M KOH in ^{i}PrOH

Run	Substrate[a]	Base (M)	Conversion (%)[b]		
			1 h	3 h	24 h
1	A	0.2	8	21	75
2	C	0.2	21	51	98
3	A	0.02	6	34	94
4	B	0.02	4	18	94
5	C	0.02	50	83	>99

10 mL of KOH in ^{i}PrOH, 0.1 mol % catalyst loading, 2 mmol of substrate, 84 °C

[a] A—acetophenone, B—benzophenone, C—cyclohexanone

[b] Measured by NMR integration

Catalytic studies

A preliminary investigation was carried out with [$RuCl_2\{\eta^6$-*p*-cymene$\}$**L**] to assess its activity in the transfer hydrogenation of ketones. The results of our preliminary investigations, using standard literature procedures,[2] are summarised in Table 1. The reactions were carried out at 84 °C, and the resulting conversions were recorded at 1, 3 and 24 h intervals and were determined by the relative integration of the substrates against products in their ^1H NMR spectra (see experimental section for details). Our initial catalytic reactions (runs 1 and 2) were performed using 10 mL of 0.2 M solution of KOH in ^{i}PrOH. As shown, the complex was found to be an active catalyst for the transfer hydrogenation of acetophenone and cyclohexanone. The results show that cyclohexane is hydrogenated more readily than acetophenone, as is typically found. In our previous report, we had highlighted the background catalytic activity of the base (KOH) [43], and other groups have also described similar observations [78–80]. We therefore investigated the activity

[2] We found that removal of the solvents by evaporation according to standard methods led to significant variations in the ratio of substrate to product. These variations were significant particularly in the case of cyclohexanone and cyclohexanol. Accordingly, the reaction solvent was not removed, and a solvent suppression ^1H NMR experiment was performed on the reaction mixture. This method was calibrated, at several designated ratios, by measuring the relative integration of substrates to products under the same concentrations as used for the catalytic reactions. Furthermore, all flasks were thoroughly cleaned with aqua regia and subsequently thoroughly washed with water and acetone prior to performing the catalytic tests.

at lower base concentrations; runs 3–5. The results reveal that under these conditions, the conversion of the three ketones, acetophenone, benzophenone and cyclohexanone, to the respective alcohols is essentially complete within a 24-h period at very low catalyst loadings (0.1 mol %). This activity is comparable to other known ruthenium–cymene complexes [26–31]. Furthermore, the results even show that overall the catalysts perform better at these lower base concentrations, suggesting that in this case, the base is involved in catalyst deactivation. Run 5 reveals a significant conversion (50 %) of cyclohexanone to cyclohexanol within the first hour.

Conclusions

In summary, we have investigated a series of ruthenium complexes in our search for suitable and active ruthenium catalysts containing the ligand diphenyl-2-(3-methyl)indolylphosphine (**L**). Two such complexes have been structurally characterised. The title complex, [$RuCl_2\{\eta^6$-*p*-cymene$\}$**L**], was synthesised in good yield and was fully characterised by spectroscopic and analytical methods. It was also found to be an active catalyst for the transfer hydrogenation of acetophenone, benzophenone and cyclohexanone, even at low catalyst loading and low-base concentration (0.1 mol % catalyst and 0.02 M KOH in iPrOH). The activities are comparable to other ruthenium complexes at similar catalyst loadings; however, there is little evidence for a significant enhancement based on the presence of the N–H functional group.

Experimental section

General remarks

All manipulations were performed by using standard Schlenk techniques. Solvents (CH_2Cl_2, MeCN and hexane) were dried using a Grubbs' alumina system and were kept in Young's ampoules under N_2 over molecular sieves (4 Å). The ligand, **L** [44], was synthesised according to the literature procedures. The deuterated solvent, $CDCl_3$, was degassed by three freeze–thaw cycles, stirred over 4 Å molecular sieves, then vacuum distilled and stored in Young's ampoules over 4 Å molecular sieves under N_2. ^{1}H NMR, $^{31}P\{^1H\}$ NMR spectra were recorded on a JEOL Lambda 300 spectrometer operating at 300 MHz (^{1}H), a JEOL ECP300 spectrometer operating at 300 MHz (^{1}H) or a JEOL ECP 400 spectrometer operating at 400 MHz (^{1}H). $^{13}C\{^1H\}$ NMR, DEPT-135 and heteronuclear correlation experiments spectra were recorded on a JEOL ECP400 spectrometer operating at 400 MHz (^{1}H), or a Varian 400-MR spectrometer operating at 400 MHz (^{1}H). The spectra were referenced internally, to the residual protic solvent (^{1}H) or the signals of the solvent (^{13}C). $^{31}P\{^1H\}$ NMR spectra are referenced relative to high frequency of 85 % H_3PO_4. Mass spectra were recorded on a Bruker Daltonics Apex (7.0 Tesla) FT-ICR-MS mass spectrometer using ESI^+ ionisation. Elemental analyses were performed at the microanalytical laboratory of the School of Chemistry at the University of Bristol. Infrared spectra were recorded on a Perkin-Elmer Spectrum 100 FT-IR spectrometer (solid state, neat) from 4,000 to 650 cm^{-1}. Figure 4 provides the numbering scheme used to assign the ^{1}H and $^{13}C\{^1H\}$ NMR spectra.

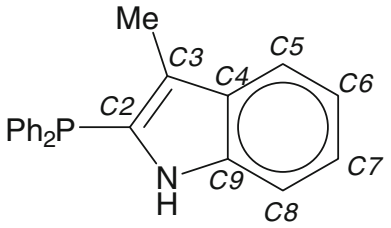

Fig. 4 Numbering scheme for **L**

Reaction of $Ru(PPh_3)_3Cl_2$ with fivefold excess of **L**

A Schlenk flask was charged with dichloro-tris(triphenylphosphine)ruthenium (10.0 mg, 0.010 mmol) and **L** (16.4 mg, 0.052 mmol). Toluene (5 mL) was subsequently added to the mixture. The resulting brown solution gradually turned to yellow after stirring at room temperature overnight. An orange powder was precipitated when hexane (10 mL) was added into the concentrated mixture. The product was isolated by filtration and then dissolved in acetonitrile. Yellow crystals suitable for single-crystal X-ray diffraction study were grown from slow evaporation of the acetonitrile solution. $^{31}P\{^1H\}$ NMR of sample prior to exposure to MeCN ($CDCl_3$, 121.7 MHz) δ [ppm] = 28.4 (br, $\Delta\nu_{1/2}$ = 66 Hz), 35.4 (br, $\Delta\nu_{1/2}$ = 162 Hz). MS of crystalline material: ESI^+; 767.1 $[RuCl\mathbf{L}_2]^+$, 808.1 $[RuCl(MeCN)\mathbf{L}_2]^+$.

Dichloro(η^6-*p*-cymene){diphenyl(3-methyl-2-indolyl)phosphine}ruthenium(II), $RuCl_2\{\eta^6$-*p*-cymene$\}$**L**

A Schlenk flask was charged with di-μ-chloro{chloro(η^6-p-cymene)ruthenium} dimer (50.0 mg, 0.081 mmol) and **L** (103.0 mg, 0.326 mmol). DCM (10 mL) was subsequently added to the mixture. The resulting red solution was stirred at room temperature for 3 h. A red–orange powder was precipitated when hexane (10 mL) was added into the concentrated (2 mL) mixture. The product was isolated by filtration and then dried under vacuum (59.8 mg, 0.096 mmol, 59 %). Red crystals suitable for single-crystal X-ray diffraction study were grown from layering hexane

upon DCM solution. ^{1}H NMR ($CDCl_3$, 400.2 MHz) δ [ppm] = 0.98 (d, $^{3}J_{HH}$ = 7.1 Hz, 6H, $^{cy}CH(CH_3)_2$), 1.75 (d, $^{4}J_{PH}$ = 1.2 Hz, 3H, $^{indole}CH_3$), 1.83 (s, 3H, $^{cy}CH_3${ring}), 2.70 (sept, $^{3}J_{HH}$ = 7.0 Hz, 1H, $^{cy}CH(CH_3)_2$), 5.15 (d, $^{3}J_{HH}$ = 6.4 Hz, 2H, $^{cy}C^{2,6}H$), 5.18 (dd, $^{3}J_{HH}$ = 6.3 Hz, $^{4}J_{HH}$ = 1.3 Hz, 2H, $^{cy}C^{3,5}H$), 7.00 (ddd, $^{3}J_{HH}$ = 7.9 Hz, $^{3}J_{HH}$ = 7.1 Hz, $^{4}J_{HH}$ = 0.9 Hz, 1H, $^{indole}C^{6}H$), 7.17 (ddd, $^{3}J_{HH}$ = 7.6 Hz, $^{3}J_{HH}$ = 7.2 Hz, $^{4}J_{HH}$ = 0.6 Hz, 1H, $^{indole}C^{7}H$), 7.38 (ddd, $^{3}J_{HH}$ = 8.3 Hz, $^{4}J_{HH}$ = 0.9 Hz, $^{4}J_{HH}$ = 0.9 Hz, 1H, $^{indole}C^{5}H$), 7.41–7.48 (m, 7H, *o,p*-^{PPh2}CH & $^{indole}C^{8}H$), 7.92–8.04 (m, 4H, *m*-^{PPh2}CH), 10.44 (br, 1H, N*H*). ^{31}P {^{1}H} NMR ($CDCl_3$, 121.7 MHz) δ [ppm] = 9.48 (s, PPh_2). ^{13}C {^{1}H} NMR ($CDCl_3$, 100.5 MHz) δ [ppm] = 10.8 (s, $^{indole}CH_3$), 17.3 (s, $^{cy}CH_3${ring}), 21.6 (s, $^{cy}CH(CH_3)_2$), 30.2 (s, $^{cy}CH(CH_3)_2$), 85.8 (d, J_{PC} = 5.5 Hz, $^{cy}C^{2,6}H$), 90.7 (d, J_{PC} = 3.9 Hz, $^{cy}C^{3,5}H$), 94.9 (s, $^{cy}C^{4}CH_3$), 110.5 (d, J_{PC} = 1.6 Hz, $^{cy}C^{1}CHMe_2$), 112.2 (s, $^{indole}C^{5}H$), 118.7 (s, $^{indole}C^{8}H$), 118.8 (s, $^{indole}C^{6}H$), 119.0 (d, $^{1}J_{CP}$ = 1.6 Hz, $^{indole}CPPh_2$), 122.2 (s, $^{indole}CCH_3$), 123.3 (s, $^{indole}C^{7}H$), 128.3 (d, $^{2}J_{CP}$ = 10.9 Hz, *o*-^{PPh2}CH), 128.6 (d, $^{3}J_{CP}$ = 8.6 Hz, $^{indole}C^{4}$), 130.5 (d, $^{4}J_{CP}$ = 2.3 Hz, *p*-^{PPh2}CH), 132.8 (d, $^{3}J_{CP}$ = 9.3 Hz, *m*-^{PPh2}CH), 133.1 ($^{PPh2}C_{ipso}$), 136.8 (d, $^{3}J_{CP}$ = 9.3 Hz, $^{indole}C^{9}$). MS(ESI): m/z 550.13 [M-2Cl$^-$ + H$^+$]$^+$ (100 %), 586.10 [M-Cl$^-$]$^+$ (25 %), 644.06 [M + Na$^+$]$^+$ (95 %). Anal. Calcd. for $C_{31}H_{32}Cl_2NPRu$ (621.54): C, 59.90; H, 5.19; N, 2.25. Found: C, 59.71; H, 5.02; N, 2.60. IR(cm^{-1}): 3289.1 $\upsilon_{(N-H)}$.

Catalyst screening

The catalytic reactions were performed in a Radleys carousel as follows: A CH_2Cl_2 solution containing 0.1 mol % of $RuCl_2\{\eta^6$-*p*-cymene$\}$**L** was transferred to a Teflon screw top tube which was connected to a Schlenk line. The solvent was then evaporated under reduced pressure. 2 mmol of substrate (acetophenone, 157 μL; benzophenone, 364 mg; cyclohexanone, 207 μL) was added, followed by 10 mL of a 0.2 M (high-base conditions) or a 0.02 M (low-base conditions) solution of KOH in ^{i}PrOH via a syringe, and the mixture was heated to 84 °C. The reaction was sampled at 1, 3 and 24 h, and the portion was added into an NMR tube without evaporation or filtration. Three drops of D_2O were added into the NMR tube, and the residue analysed by ^{1}H NMR in $CDCl_3$ (with a reaction mixture: $CDCl_3$ ratio of 2: 3 by volume). The percentage conversions were determined by relative integration of characteristic resonances of both the products and the starting materials.

X-ray crystallography

X-ray diffraction experiments on $[Ru_2Cl_4(NCMe)\mathbf{L}_4]$ and $[RuCl_2\{\eta^6$-*p*-cymene$\}$**L**] were carried out at 100 K on a Bruker APEX II diffractometer using Mo–K_α radiation (λ = 0.71073 Å) source. Data collections were performed using a CCD area detector from a single crystal mounted on a glass fibre. Intensities were integrated [81] from several series of exposures measuring 0.5° in ω or φ. Absorption corrections were based on equivalent reflections using SADABS [82]. Structures were solved using ShelLXS and refined against all F_o^2 data with hydrogen atoms riding in calculated positions using ShelXL [83]. Crystal structure and refinement data are given in Table 2. For $[Ru_2Cl_4(NCMe)\mathbf{L}_4]$, the crystal model contained residual electron density which could not be identified. Thus, the data were modelled with the SQUEEZE algorithm as implemented in PLATON, which calculated an extra 45 electrons per complex. This most likely correlates with an extra molecule of DCM per molecule of complex. For $[RuCl_2\{\eta^6$-*p*-cymene$\}$**L**], the crystal model contained two independent complexes in the unit cell. One of these complexes contained disorder in **L**. Figures 2, 3 and the graphical abstract have been generated using ORTEP [84] and POV-Ray software [85]. CCDC 936150 [$RuCl_2\{\eta^6$-*p*-

Table 2 Crystal structure and refinement data for $[Ru_2Cl_4(NCMe)\mathbf{L}_4]$ and $RuCl_2\{\eta^6$-*p*-cymene$\}$**L**

Compound	$[Ru_2Cl_4(NCMe)\mathbf{L}_4]$	$RuCl_2\{\eta^6$-*p*-cymene$\}$**L**
Colour, habit	Orange prism	Red rod
Size/mm	0.16 × 0.08 × 0.08	0.12 × 0.10 × 0.06
Empirical formula	$C_{88}H_{77}Cl_{10}N_5P_4Ru_2$	$C_{31}H_{32}Cl_2NPRu$
M	1,885.07	621.52
Crystal system	Monoclinic	Monoclinic
Space group	*P*21/*n*	*P*21/*c*
a/Å	14.8514(10)	22.333(4)
b/Å	20.8694(16)	15.4163(18)
c/Å	27.755(2)	17.224(3)
α/°	90.00	90.00
β/°	97.320(4)	111.901(16)
γ/°	90.00	90.00
V/Å^3	8,532.2(11)	5,502.1(16)
Z	4	8
μ/mm^{-1}	0.790	0.844
T/*K*	100	100
$\theta_{min,max}$	1.22, 27.60	3.55, 25.36
Completeness	0.988 to θ = 27.60°	0.995 to θ = 25.36°
Reflections: total/independent	19592/19592	100233/10038
R_{int}	0.0000	0.1035
Final *R*1 and *wR*2	0.0722, 0.2032	0.0576, 0.1682
Largest peak, hole/e Å^{-3}	1.251, −1.314	0.724, −0.917
ρ_{calc}/g cm^{-3}	1.467	1.501

cymene}**L**]) and 936151 ([Ru_2Cl_4(NCMe)$\mathbf{L}_4$]) contain the supplementary crystallographic data for this paper. These data can be obtained free of charge from The Cambridge Crystallographic Data Centre via www.ccdc.cam.ac.uk/data_request/cif.

Acknowledgments The authors thank the Royal Society for a Royal Society Dorothy Hodgkin Research Fellowship for GRO and Johnson Matthey for the generous loan of ruthenium salts.

References

1. Ikariya T (2011) Bull Chem Soc Jpn 84:1
2. Chidambaram G, Milstein D (2011) Acc Chem Res 44:588
3. Dub PA, Ikariya T (2012) ACS Catal 2:1718
4. Zhao B, Han Z, Ding K (2013) Angew Chem Int Ed 52:4744
5. Doucet H, Ohkuma T, Murata K, Yokozawa T, Kozawa M, Katayama E, England AF, Ikariya T, Noyori R (1998) Angew Chem Int Ed 37:1703
6. Yamakawa M, Ito H, Noyori R (2000) J Am Chem Soc 122:1466
7. Sandoval CA, Ohkuma T, Muñiz K, Noyori R (2003) J Am Chem Soc 125:13490
8. Clapham SE, Hadzovic A, Morris RH (2004) Coord Chem Rev 248:2201
9. Chowdhury RL Bäckvall J-E (1991) J Chem Soc Chem Commun 1063–1064
10. MacInnis MC, MacLean DF, Lundgren RJ, McDonald R, Turculet L (2007) Organometallics 26:6522
11. Gladiali S, Alberico E (2006) Chem Soc Rev 35:226
12. Amoroso D, Jabri A, Yap GPA, dos Gusev DG, Santos EN, Fogg DE (2004) Organometallics 23:4047
13. Zweifel T, Naubron J-V, Büttner T, Ott T, Grötzmache H (2008) Angew Chem Int Ed 47:3245
14. Samec JSM, Bäckvall J-E, Andersson PG, Brandt P (2006) Chem Soc Rev 35:237
15. Zeng F, Yu Z (2008) Organometallics 27:2898
16. Clarke ZE, Maragh PT, Dasgupta TP, Gusev DG, Lough AJ, Addur-Rashid K (2006) Organometallics 25:4113
17. Baratta W, Herdtweck E, Siega K, Toniutti M, Rigo P (2005) Organometallics 24:1660
18. Zotto AD, Baratta W, Ballico M, Herdtweck E, Pigo P (2007) Organometallics 26:5636
19. Zhao M, Yu Z, Yan S, Li Y (2009) J Organomet Chem 694:3068
20. Zhao M, Yu Z, Yan S, Li Y (2009) Tetrahedron Lett 50:4624
21. Zeng F, Yu Z (2009) Organometallics 28:1855
22. Rahman MS, Prince PD, Steed JW, Hii KK (2002) Organometallics 21:4927
23. Crochet P, Gimeno J, Borge J, García-Granda S (2003) New J Chem 27:414
24. de Araujo MP, de Figueiredo AT, Bogado AL, Poelhsitz GV, Ellena J, Castellano EE, Donnici CL, Comasseto JV, Batista AA (2005) Organometallics 24:6159
25. Lau CP, Ng SM, Jia G, Lin Z (2007) Coord Chem Rev 251:2223
26. Aznar R, Grabulosa A, Mannu A, Muller G, Sainz D, Moreno V, Font-Bardia M, Calvet T, Lorenzo J (2013) Organometallics 32:2344
27. Bennett MA, Smith AK (1974) J Chem Soc Dalton Trans 233–241
28. Carriedo GA, Crochet P, García Alonso FJ, Gimeno J, Presa-Soto A (2004) Eur J Inorg Chem 3668–3674
29. Wang L, Yang Q, Fu H-Y, Chen H, Yuan M-L, Li R-X (2011) Appl Organomet Chem 25:626
30. Grabulosa A, Mannu A, Mezzetti A, Muller G (2012) J Organomet Chem 696:4221
31. Grabulosa A, Mannu A, Alberico E, Denurra S, Gladiali S, Muller GJ (2012) Mol Catal A Chem 363–364:49
32. Tsoureas N, Hamilton A, Haddow MF, Harvey JN, Orpen AG, Owen GR (2013) Organometallics 32:2840
33. Owen GR (2012) Chem Soc Rev 41:3535
34. Zech A, Haddow MF, Othman H, Owen GR (2012) Organometallics 31:6753
35. Dyson G, Zech A, Rawe BW, Haddow MF, Hamilton A, Owen GR (2011) Organometallics 30:5844
36. Tsoureas N, Kuo Y–Y, Haddow MF, Owen GR (2011) Chem Commun 47:484
37. Tsoureas N, Bevis T, Butts CP, Hamilton A, Owen GR (2009) Organometallics 28:5222
38. Rudolf GC, Hamilton A, Orpen AG, Owen GR (2009) Chem Commun 533–555
39. Owen GR, Tsoureas N, Hamilton A, Orpen AG (2008) Dalton Trans 6039–6044
40. Owen GR, Tsoureas N, Hope RF, Kuo Y-Y, Haddow MF (2011) Dalton Trans 40:5906
41. Tsoureas N, Nunn J, Bevis T, Haddow MF, Hamilton A, Owen GR (2011) Dalton Trans 40:951
42. Tsoureas N, Hope RF, Haddow MF, Owen GR (2011) Eur J Inorg Chem 5233–5241
43. Kuo Y-Y, Haddow MF, Perez-Redondo A, Owen GR (2010) Dalton Trans 39:6239
44. Yu JO, Lam E, Sereda JL, Rampersad NC, Lough AJ, Browning CS, Farrar DH (2005) Organometallics 24:37
45. Lam E, Farrar DH, Browning CS, Lough AJ (2004) Dalton Trans 3383–3388
46. Yu JO, Browning CS, Farrar DH (2008) Chem Commun 1020–1022
47. Koshevoy IO, Shakirova JR, Melnikov AS, Haukka M, Tunik SP, Pakkanena TA (2011) Dalton Trans 40:7927
48. Berens U, Brown JM, Long J, Selke R (1996) Tetrahedron Asymmetry 7:285
49. Artemova NV, Chevykalova MN, Luzikov YN, Nifant'ev IE, Nifant'ev EE (2004) Tetrahedron 60:10365
50. So CM, Yeung CC, Lau CP, Kwong FY (2008) J Org Chem 73:7803
51. Wassenaar J, Kuil M, Reek JNH (2008) Adv Synth Catal 350:1610
52. Wassenaar J, Reek JNH (2007) Dalton Trans 3750–3753
53. Wassenaar J, van Zutphen S, Mora G, Le Floch P, Siegler MA, Spek AL, Reek JNH (2009) Organometallics 28:2724
54. Ciaridge TDW, Long JM, Brown JM, Hibbs D, Hursthouse MB (1997) Tetrahedron 53:4035
55. Penno D, Koshevoy IO, Estevan F, Sana M, Ubeda MA, Pérez-Prieto J (2010) Organometallics 29:703
56. Bauer RC, Gloaguen Y, Lutz M, de Reek JNH, van der Bruina B, Vlugt JI (2011) Dalton Trans 40:8822
57. Bonet A, Gulyás H, Koshevoy IO, Estevan F, Sanaú M, Úbeda MA, Fernández E (2010) Chem Eur J 16:6382
58. Kondoh A, Yorimitsu H, Oshima K (2010) Org Lett 12:1476
59. Noyori R, Hashiguchi S (1997) Acc Chem Res 30:97
60. Zeng F, Yu Z (2008) Organometallics 27:2898
61. Uson R, Oro LA, Sariego R, Esteruelas MA (1981) J Organomet Chem 214:399
62. Zanotti-Gerosa A, Hems W, Groarke M, Hancock F (2005) Platin Met Rev 49:158
63. Gilbert JD, Wilkinson G (1969) J Chem Soc (A) 1749–1753
64. Jung CW, Garrou PE, Hoffman PR, Caulton KG (1984) Inorg Chem 23:726
65. Fogg DE, James BR (1997) Inorg Chem 36:1961

66. Joshi AM, Thorburn IS, Rettig JS, James BR (1992) Inorg Chim Acta 198–200:283
67. Amoroso D, Yap GPA, Fogg DE (2001) Can J Chem 79:958
68. Getty AD, Tai C-C, Linehan JC, Jessop PG, Olmstead MM, Rheingold AL (2009) Orgamometallics 28:5466
69. da Silva AC, Piotrowski H, Mayer P, Polborn K, Severin K (2001) Eur J Inorg Chem 685–691
70. Cotton FA, Torralba RC, Matusz M (1991) Inorg Chem 30:2196
71. Mothes E, Sentets S, Luquin MA, Mathieu R, Lugan N, Lavigne G (2008) Organometallics 27:1193
72. Yang L, Krüger A, Neels A, Albrecht M (2008) Organometallics 27:3161
73. Herberhold M, Yan H, Milius W (2000) J Organomet Chem 598:142
74. Hodson E, Simpson SJ (2004) Polyhedron 23:2695
75. Bruno G, Panzalorto M, Nicoló F, Arena CG, Cardiano P (2000) Acta Crystallogr C 56:e429
76. Hafner A, der Miihlebach A, Schaaf PA (1997) Angew Chem Int Ed Eng 36:2121
77. Immirzi A, Musco A (1977) Inorg Chim Acta 25:L41
78. Carrión MC, Jalón FA, Manzano BR, Rodríguez AM, Sepúlveda F, Maestro M (2007) Eur J Inorg Chem 3961–3973
79. Le Page MD, James BR (2000) Chem Commun 1647–1648
80. Bertoli M, Choualeb A, Gusev DG, Lough AJ, Major Q, Moore B (2011) Dalton Trans 40:8941
81. Bruker-AXS SAINT V7.60A
82. Sheldrick GM SADABS V2008/1-2, University of Göttingen, Germany
83. Sheldrick GM (2008) Acta Cryst A 64:112
84. Farrugia LJ (1997) ORTEP-3 for Windows v2.02. J Appl Cryst 30:565
85. POV-Ray for Windows v3.6.2, Persistence of Vision Pty. Ltd., 2004, computer software, retrieved from http://www.povray.org/download/